Journal of
Powder Metallurgy & Mining
ISSN: 2168-9806

Ali et al., J Powder Metall Min 2017, 6:1
DOI: 10.4172/2168-9806.1000163

Research Article OMICS International

Structural, Magnetic and Dielectric Properties of Sm^{3+} and Mn^{2+} Co-doped $BiFeO_3$ Nanoparticles

Ali SI[1,2]*, Kiani M[2] and Rizwan S[2]

[1]*State Key Laboratory for New Ceramics & Fine Processing, School of Materials Science & Engineering, Tsinghua University, Beijing 100084, PR China*
[2]*Department of Physics, School of Natural Science (SNS), National University of Science & Technology (NUST), Islamabad 44000, Pakistan*

Abstract

The structural, morphological, magnetic and dielectric properties of Samarium (Sm^{3+}) and Manganese (Mn^{2+}) doped Bismuth ferrite (BSFMO, Sm=5% and Mn=0%, 5%, 10%, 20%, 25%) nanoparticles are presented which were characterized by X-ray diffraction (XRD), scanning electron microscope (SEM), superconducting quantum interference device (SQUID) and LCR meter, respectively. The XRD and SEM measurement show that the nanoparticles were successfully synthesized by an improved sol-gel technique. The nanoparticles size decreases with increase in the Mn^{2+} concentration. The dielectric measurement revealed that the dielectric constant and dielectric loss decreases at higher frequency. The saturation magnetization and the magnetic coercivity of Mn-doped BSFO decrease by increasing Mn concentration which is attributed to the increase in $Bi_2Mn_4O_9$ antiferromagnetic impurity phase and the increase in antiferromagnetic spin wavelength. Our results suggest that the resulting nano-composite is a soft ferromagnetic material and is a suitable candidate for magnetic sensors operable at room-temperature.

Keywords: Nanoparticles; Dielectric dispersion; Antiferromagnetic impurity

Introduction

$BiFeO_3$ (BFO) is one of the multiferroics with coexistence of antiferromagnetic and ferroelectric order parameters simultaneously in perovskite structure [1,2]. BFO is an antiferromagnetic material with Neel temperature of about 370°C and ferroelectric material with the Curie temperature of 830°C [3,4]. The multiferroic materials are explored widely due to potential applications such as in microwave devices, satellite communication, memory devices, audio–video devices, digital recording, sensors and spintronic devices [5,6]. Therefore, $BiFeO_3$ is considered to be as a primary contestant for magnetoelectric applications at room temperature. It belongs to R3c space group and has a rhombohedral distorted structure [7]. The magnetic behavior of $BiFeO_3$ owed to partially filled 3d orbital electrons of Fe^{3+} ions that lead to G-type anti ferromagnetism and the ferroelectric property which originates from Bi-O hybridization due to stereo chemical activity of Bi6s2 lone pair [8].

As, BFO has a small band-gap (2.2 eV) so, it has got more attraction for the reason that it is possible to be employed as an efficient visible-light photo catalyst. Therefore, BFO-based photo catalysts are very reactive to visible-light and exhibit higher photo catalytic efficiency in visible range compared to the TiO_2-based photo catalysts. To further improve the photo catalytic Performance, efforts have been made for band-gap engineering by different elemental doping onto the BFO lattice sites [9]. In order to prepare BFO nanoparticles of small sizes (<60 nm), several alternative chemical synthesis routes were adopted such as ferrioxalate precursor method [10], micro-emulsion technique [11], citrate-gel method [12], sol–gel method [8,13], co-precipitation method, soft chemical route, etc. Recently, many elements like Gd^{3+}, La^{3+}, Mn^{2+}, Co^{2+}, co-doped La^{3+} and Co^{2+}, La^{3+} and Mn^{2+} have been doped onto BFO in order to improve its morphology, electrical and magnetic properties [14-23].

In the present work, Bi^{3+} and Fe^{3+}cations of $BiFeO_3$ were replaced by Sm^{3+} and Mn^{2+} respectively in order to study the dielectric and magnetic properties of the resulting nanoparticle compound. The Sm^{3+} and Mn^{2+} ions were introduced in A-site and B-site onto BFO, respectively. In this research, an effort is made to study the behavior of BSFMO (Sm=5% and Mn=0%, 5%, 10%, 20%, 25%) nanoparticle system including, physical, structural, magnetic and dielectric parameters at room temperature.

Experimental Section

Pure and co-doped BFO were prepared by an improved sol-gel method. The $Bi_{1-x}Sm_xFe_{1-y}Mn_yO_3$ (BSFMO, x=0, 0.05; y=0, 0.05, 0.1, 0.15, 0.2, 0.25) nanoparticles abbreviated as BSFO, BSFMO-5, BSFMO-10, BSFMO-20, and BSFMO-25, respectively. The samarium nitrate hex hydrate and bismuth nitrate pent hydrate dissolved in acetic acid were added to ethylene glycol and stirred for 2 h at room temperature. Manganous nitrate solution and iron nitrate nonahydrate powder were dissolved in acetic acid and constantly stirred for 1 h. Hereafter, both solutions were mixed and stirred for 2 h. A homogeneous, reddish brown solution was produced and was dried at 80°C to obtain a dry gel and then calcined at 600°C for 3 h. In the experimental process, acetic acid was used as the catalyst in the sol system and the hydrolysis speed controls the concentration during synthesis process; ethylene glycol used as solvent during hydrolysis can keep the different electronegativity of bismuth (Bi^{3+}) and iron (Fe^{3+}) and a stable solution is formed by its linearly structured molecule [24]. The structural analysis of the BSFMO samples was carried out by X-ray Diffractometer (XRD) in the range of 20~80 with Cu-Ka radiation working at 40 kV and 26 mA. Scanning electron microscope (SEM) and energy dispersive spectrometer (EDS) were used for morphological analysis and to examine the chemical composition of the BSFMO samples, respectively. The LCR meter was used to study the dielectric properties of pure and Sm^{3+} and Mn^{2+} co-

***Corresponding author:** Ali SI, State Key Laboratory for New Ceramics & Fine Processing, School of Materials Science and Engineering, Tsinghua University, Beijing 100084, PR China, Tel: +86-10-62782770; E-mail: irfansyed715@gmail.com

Received March 17, 2017; **Accepted** March 22, 2017; **Published** March 31, 2017

Citation: Ali SI, Kiani M, Rizwan S (2017) Structural, Magnetic and Dielectric Properties of Sm^{3+} and Mn^{2+} Co-doped $BiFeO_3$ Nanoparticles. J Powder Metall Min 6: 163. doi:10.4172/2168-9806.1000163

Copyright: © 2017 Ali SI, et al. This is an open-access article distributed under the terms of the Creative Commons Attribution License, which permits unrestricted use, distribution, and reproduction in any medium, provided the original author and source are credited.

Citation: Ali SI, Kiani M, Rizwan S (2017) Structural, Magnetic and Dielectric Properties of Sm^{3+} and Mn^{2+} Co-doped $BiFeO_3$ Nanoparticles. J Powder Metall Min 6: 163. doi:10.4172/2168-9806.1000163

doped BFO nanoparticles. The Superconducting quantum interference device (SQUID) was used to study the ferromagnetic properties of the samples.

Results and Discussion

Structural and morphological characterizations of BFO and BSFMO nanoparticles

Figure 1 shows XRD patterns of the Sm^{3+} and Mn^{2+} co-doped BFO nanoparticles calcined in air at 600°C. The XRD pattern of pure BFO corresponds to the distorted rhombohedral structure with an R3c space group (JCPDS card no. 20-0169). By further increasing Mn^{2+} doping concentration onto BFO sites, an additional peak of an impurity phase of $Bi_2Fe_4O_9$ is nearly removed, as is reported in previous report [25]. The SEM images of the BSFMO samples calcined at 600°C are shown in Figure 2. The particle size of BSFMO reduces (57-19 nm) by increasing concentration of Mn^{2+} doping. Hence, the variation in the grain morphology of BSFMO nanoparticles is attributed to the addition of Mn^{2+} at the Fe^{3+} sites, as the Mn^{2+} concentration further increases to 25 mol% in BSFO, the particles were agglomerated and undergo a phase transition from rhombohedral to orthorhombic phase [26,27]. The reduction in grain size may be attributed to the difference in the ionic radius of Bi^{3+} and Sm^{3+} as well as the difference in bond strength which is almost 1.8 times greater for Sm–O bond (619 ± 13 kJ/mol) than the Bi–O bond (343 ± 6 kJ/mol). The Kirkendall effect may be the another cause for decrease of grain size due to doping which arise due to diffusion rates of constituting elements of the compounds [28].

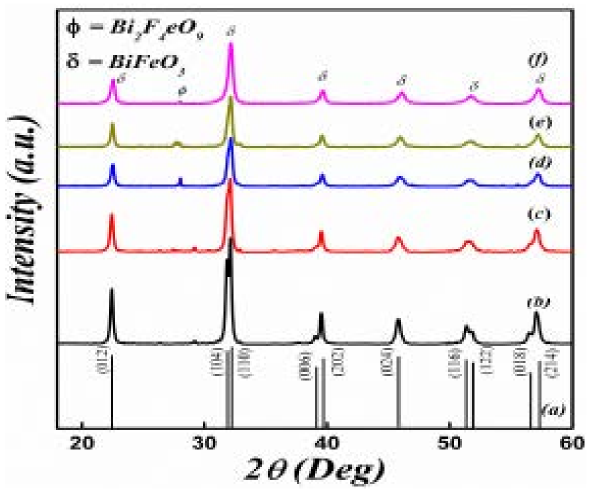

Figure 1: The XRD patterns of pure BFO and Sm and Mn co-doped BFO nanoparticles (a) BFO (b) BSFO (c) BSFMO-5Mn (d) BSFMO-10Mn (e) BSFMO-20Mn (f) BSFMO-25Mn.

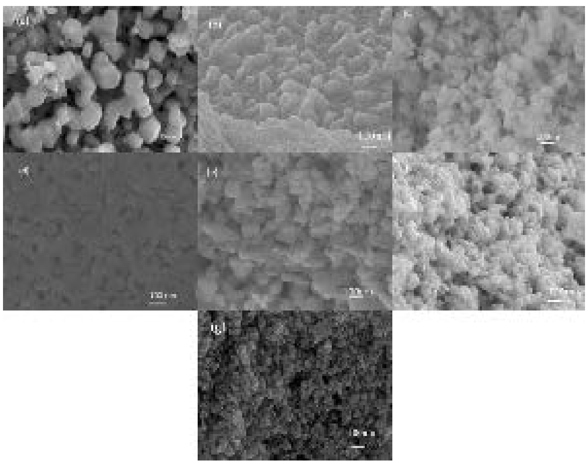

Figure 2: The SEM images of pure BFO and various Sm and Mn co-doped BFO nanoparticles (a) BFO (b) BSFO (c) BSFMO-5 (d) BSFMO-10 (e) BSFMO-15 (f) BSFMO-20 (g) BSFMO-25.

Dielectric properties: Figure 3a shows the variation of dielectric constant vs. frequency obtained for pure BFO and BSFMO samples, measured at room temperature, with different Mn^{2+} doping concentration under the frequency range of 20 MHz -120 MHz (Figure 3a and 3b). From Figure 3, it can be seen that the dielectric constant decreases with increase in the frequency. The observed behavior of BSFMO nanoparticles can be attributed to the space charge relaxation effect on the basis of polarization and hopping conduction processes in nanoparticles [29]. As, both dielectric constant 'ε' (real part) and dielectric loss 'ε' account for charge storage capacity/polarization ability and energy dissipation; it is observed that the dielectric constant is decreased rapidly by increasing frequency and become independent at high frequency range. The decrement of real part is ascribed to the dielectric relaxation. Koop's theory describes the phenomena of dielectric dispersion. According to this theory, the decrement in real part with increasing frequency is attributed to the fact that atoms in the dielectric material required a finite time to align up along their axis in the direction of applied field. The frequency of the applied electric field increases and a point is reached when dipoles do not follow the frequency of the applied electric field and value of the real part is decreased. With further increase in the frequency of the applied field, the polarization would hardly move before the field reverses its

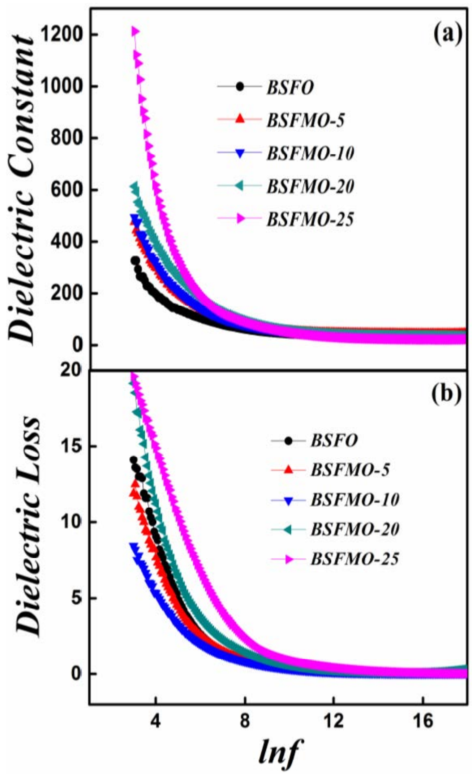

Figure 3: Variation of (a) dielectric constant and (b) dielectric loss, as a function of frequency for BSFMO samples with different Mn concentration.

Citation: Ali SI, Kiani M, Rizwan S (2017) Structural, Magnetic and Dielectric Properties of Sm^{3+} and Mn^{2+} Co-doped $BiFeO_3$ Nanoparticles. J Powder Metall Min 6: 163. doi:10.4172/2168-9806.1000163

direction and makes no role in polarization thus, becomes independent at high frequency range. The decrement in dielectric constant is associated with the hopping of the electrons from Fe^{2+} to Fe^{3+} ions. Moreover, at low frequency, electric field does not provide sufficient energy to electron for hopping but as we increase the frequency of electric field, it provides sufficient energy and a specific point is reached when hopping of electron is started from Fe^{2+} to Fe^{3+} ions. Therefore, the conductivity of the dielectric increases with frequency [30]. The dielectric constant of co-doped BFO nanoparticles is larger than that of un-doped BFO nanoparticles. This dielectric behavior of doped BFO can be explained in terms of oxygen vacancies and displacement of Fe^{3+} ions as there are always some oxygen vacancies in undoped BFO which results in relatively high conductivity and less dielectric constant. The dielectric loss data shows that the dielectric loss follows the same trend as for the dielectric constant. In the low-frequency region, there is a greater dielectric loss due to increased resistivity owing to the accumulation of charges. It is expected that more oxygen vacancies would be introduced by the substitution of Mn^{2+} ions in BSFO which will increase the hopping conduction mechanism resulting in higher dielectric loss. This kind of behavior was previously reported in the Sr^{2þ} and the Pb^{2þ} doped BFO. Figure 4 shows that the ac conductivity of the BSFMO samples measured at room temperature. The Ac conductivity was calculated by the capacitance (C_p) and dissipation factor (D) as a function of frequency of the applied voltage. The overall conductivity at a specific temperature over a wide frequency range follows the universal dielectric response

Magnetic properties: Figure 5a shows the magnetization vs. magnetic field (M–H) curves of the Sm^{3+} and Mn^{2+} co-doped BFO nanoparticles measured under the magnetic field loop of ±10,000 Oe at room temperature. The BSFO shows a good magnetic hysteresis behavior due to the distorted anti-ferromagnetic spin cycloid of pure BFO and due to magnetically active Sm^{3+} characteristics. It is found that the perfect magnetic hysteresis loops were observed for each composition and that the saturation magnetization decreases with increasing Mn^{2+} concentration. It is due to the fact that the antiferromagnetic $Bi_2Fe_4O_9$ impurity phase continuously increases with increase in Mn concentration as is shown in the X-ray diffraction pattern in Figure 5a.

Figure 5b shows a significant decrease in magnetic coercivity by increasing the concentration of Mn^{2+}. BFO has largest coercivity of 222 Oe which decreases to 142 Oe in Sm^{3+} doped BFO nanoparticles. The coercivity then decreases continuously and attains the minimum value of 25Oe at 25% Mn^{2+}; the coercivity and magnetization both decrease by increasing Mn^{2+} concentration. The saturation magnetization of the BSFMO-25 nanoparticles is smaller than all other BSFMO samples with smaller Mn concentration which is due the antiferromagnetic impurity phase of $Bi_2Fe_4O_9$ as the magnetization of $Bi_2Fe_4O_9$ is almost zero at room temperature. Therefore, It is evidently observed that the magnetic properties of the samples are strongly dependent on doping concentration making the magnetic nanoparticles controllable externally.

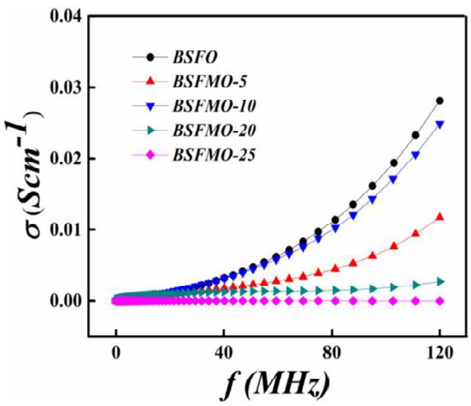

Figure 4: Frequency dependence of ac conductivity of BSFMO samples at different Mn concentration.

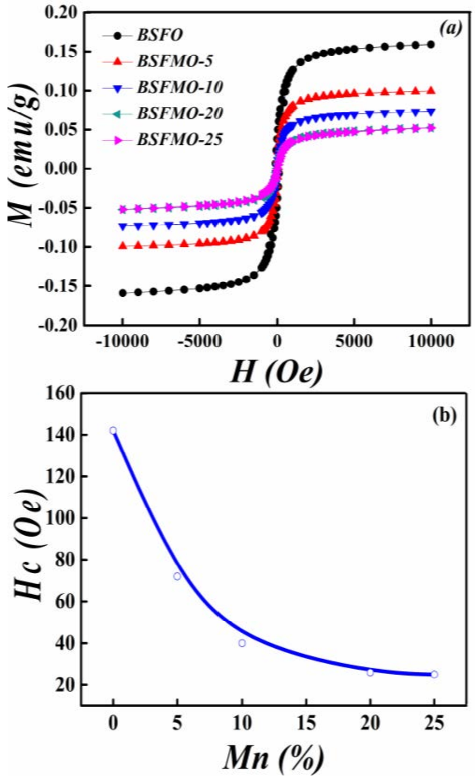

Figure 5: (a) The M–H curve and (b) magnetic coercivity variation as a function of Mn concentration for BSFMO samples.

Conclusion

In summary, pure BFO and BFSMO nanoparticles (Sm: 5% and Mn: 0%, 5%, 10%, 20%, 25%) were prepared successfully *via* improved sol-gel technique by using double solvent method and calcined at 600°C. A single phase perovskite structure of pure bismuth ferrite nanoparticles is achieved. Structural and morphological analyses revealed that there is phase transition from rhombohedral to orthorhombic by increasing Mn^{2+} concentration. Study of dielectric properties shows that the dielectric constant and dielectric loss of all samples has the same trend; it is decreased by increasing frequency towards the stable value. The magnetization of BSFMO particles has the largest value when concentration on Mn^{2+} is zero and by increasing Mn^{2+} magnetization, coercivity and squareness decrease. The increase in magnetization is attributed to the distorted anti-ferromagnetic spin cycloid of pure $BiFeO_3$ on external doping. The magnetic nanoparticle system presented here shows their potential for the application of soft magnetic materials.

Acknowledgement

The work was supported by National University of Science and Technology

(NUST), Islamabad, Pakistan, and Higher Education Commission (HEC) of Pakistan.

References

1. Smolenskii GA, Yudin VM, Sher ES, Stolypin YE (1963) Antiferromagnetic properties of some perovskites. Sov Phys J Exp Theor Phys 16: 622-624.
2. Ismilzade JG (1971) Phys Status Solidi B 46: K39-41.
3. Fischer P, Polomska M, Sosnowska I, Szymanksi M (1980) Temperature dependence of the crystal and magnetic structures of $BiFeO_3$. J Phys C 13: 1931-1940.
4. Michel C, Moreau JM, Achenbach GD, Gerson R, James WJ (1969) The atomic structure of $BiFeO_3$. Solid State Commun 7: 701-704.
5. Eerenstein W, Mathur ND, Scott JF (2006) Multiferroic and magnetoelectric materials. Nature 442: 759-765.
6. Sharma S, Singh V, Kotnala RK, Dwivedi RK (2014) Lone pairs in the off-center distortion in ferromagnetic BiMnO3. Chem Mater 13: 2892-2899.
7. Cheng ZX, Li AH, Wang XL, Dou SX, Ozawa K, et al. (1982) J Appl Phys C: Solid State Phys 15: 4835.
8. Guo RQ, Fang L, Dong W, Zhang FG, Shen MR (2010) Enhanced photocatalytic activity and ferromagnetism in Gd doped BiFeO3 nanoparticles. J Phys Chem C 114: 21390-21396.
9. Ghosh S, Dasgupta S, Sen A, Maiti HS (2005) Low temperature synthesis of bismuth ferrite nanoparticles by a ferrioxalate precursor method. Mater Res Bull 40: 2073-2079.
10. Das N, Majumdar R, Sen A, Maiti HS (2007) Nanosized bismuth ferrite powder prepared through sonochemical and microemulsion techniques. Mater Lett 61: 2100-2104.
11. Jiang QH, Nan CW (2006) Synthesis and Properties of Multiferroic La-Modified BiFeO3 Ceramics. J Am Ceram Soc 89: 2123-2127.
12. Park TJ, Papaefthymiou GC, Viescas AJ, Moodenbaugh AR, Wong SS (2007) Size-dependent magnetic properties of single-crystalline multiferroic BiFeO3 nanoparticles. Nano Lett 7: 766-772.
13. Xu J, Ke H, Jia D, Wang W, Zhou Y (2009) Low-temperature synthesis of BiFeO3 nanopowders via a sol-gel method. J Alloy Compd 472: 473-477.
14. Carvalho TT, Fernandes JRA, Cruz JP, Vidal JV, Sobolev NA, et al. (2012) Room temperature structure and multiferroic properties in Bi0.7La0.3FeO3 ceramics. J Phys Chem C 554: 97-103.
15. Kothari D, Reddy VR, Gupta A, Phase DM, Lakshmi N, et al. (2007) Study of the effect of Mn doping on the BiFeO3 system. J Phys Condens Matter 19: 1-8.
16. Uniyal P, Yadav KL (2012) Enhanced magnetoelectric properties in Bi0.95Ho0.05FeO_3 polycrystalline ceramics. J Phys Chem C 511: 149-153.
17. Yang KG, Zhang YL, Yang SH, Wang B (2010) Structural, electrical, and magnetic properties of multiferroic Bi1−xLaxFe1−yCoyO_3 thin films. J Appl Phys 107: 124109-124112.
18. Yan FX, Zhao GY, Song N, Zhao N, Chen YQ (2013) In situ synthesis and characterization of fine-patterned La and Mn co-doped BiFeO3 film. J Alloys Comp 570: 19-22.
19. Chen ZW, Hu JQ, Lu ZY, He XH (2011) Low-temperature preparation of lanthanum-doped $BiFeO_3$ crystallites by a sol-gel-hydrothermal method. Ceram Int 37: 2359-2364.
20. Irfan S, Shen Y, Rizwan S, Wang HC, Khan SB, et al. (2017) Band-Gap Engineering and Enhanced Photocatalytic Activity of Sm and Mn Doped BiFeO3 Nanoparticles. J Am Ceram Soc 100: 31-40.
21. Irfan S, Rizwan S, Shen Y, Li L, Asfandiyar, et al. (2017) The Gadolinium (Gd3+) and Tin (Sn4+) Co-doped $BiFeO_3$ Nanoparticles as New Solar Light Active Photocatalyst. Sci Rep 7: 42493-42505.
22. Irfan S, Rizwan S, Shen Y, Tomovska R, Zulfiqar S, et al. (2016) Mesoporous template-free gyroid-like nanostructures based on La and Mn co-doped bismuth ferrites with improved photocatalytic activity. RSC Adv 6: 114183-114189.
23. Mukherjee A, Basu S, Manna PK, Yusuf SM, Pal M (2014) Enhancement of multiferroic properties of nanocrystalline $BiFeO_3$ powder by Gd-doping. J Alloys Comp 598: 142-150.
24. Naik R, Nazarko JJ, Flattery CS, Venkateswaran UD, Naik VM, et al. (2009) Temperature dependence of the Raman spectra of polycrystalline Ba1−xSixTiO_3. Journal of Alloys and Compounds 475: 577-580.
25. Gupta S, Sharma A, Tomar M, Gupta V, Pal M, et al. (2012) Piezoresponse force microscopy and vibrating sample magnetometer study of single phased Mn induced multiferroic $BiFeO_3$ thin film. J Appl Phys.111: 064110.
26. Wang Y, Nan CW (2008) Site modification in BiFeO3BiFeO3 thin films studied by Raman spectroscopy and piezoelectric force microscopy. J Appl Phys 103: 114104.
27. Jun YK, Moon WT, Chang CM, Kim HS, Ryu HS, et al. (2005) Solid State Commun 135: 133-137.
28. Reetu A, Agarwal S, Sanghi, Ashima N, Ahlawat M (2012) Phase transformation, dielectric and magnetic properties of Nb doped Bi0.8Sr0.2FeO3 multiferroics. Journal of Applied Physics 111: 113917-113923.
29. Chen YJ, Wu QS, Zhao J (2009) Selective synthesis on structures and morphologies of BixFeyOz nanomaterials with disparate magnetism through time control. J Alloys Comp 487: 599-604.
30. Bhole CP (2011) Ferroelectric and Dielectric Investigations of Bismuth Ferrite (BiFeO3) Nanoceramics. Arch Appl Sci Res 3: 384-389.

Citation: Ali SI, Kiani M, Rizwan S (2017) Structural, Magnetic and Dielectric Properties of Sm^{3+} and Mn^{2+} Co-doped $BiFeO_3$ Nanoparticles. J Powder Metall Min 6: 163. doi:10.4172/2168-9806.1000163

OMICS International: Open Access Publication Benefits & Features

Unique features:

- Increased global visibility of articles through worldwide distribution and indexing
- Showcasing recent research output in a timely and updated manner
- Special issues on the current trends of scientific research

Special features:

- 700+ Open Access Journals
- 50,000+ editorial team
- Rapid review process
- Quality and quick editorial, review and publication processing
- Indexing at major indexing services
- Sharing Option: Social Networking Enabled
- Authors, Reviewers and Editors rewarded with online Scientific Credits
- Better discount for your subsequent articles

Submit your manuscript at: http://www.omicsonline.org/submission